An experimental study on three-port measurements for acoustic characterization of a perforate

Shail A. Shah[a], Hans Bodén[a], Susann Boij[a]

[a] *The Marcus Wallenberg Laboratory for Sound and Vibration Research, Department of Engineering Mechanics, KTH Royal Institute of Technology, Stockholm, SE-10044, Sweden*

Abstract

Multiple analytical, experimental, and numerical studies have been carried out on perforates to study their properties under operating conditions, resulting in varying hypothesis and models to predict their performance. The ongoing effort of providing experimental results using multiform test setups is continued in this study. Incorporating the three-port technique, the passive acoustic response of a perforated plate is studied under acoustic excitation from three directions in presence of grazing flow and high-level excitation. Similar to the in-situ method, usage of the three-port technique has an advantage of being a direct method for impedance determination and is not bound by any boundary conditions traditionally considered in presence of grazing flow. Extending the observations of previous studies, a semi-empirical model is determined for the real part of the transfer impedance of a perforate, where the characterisation of the determined impedance on the testing parameters like the Strouhal number, particle velocity, flow velocity and shear number is displayed.

Keywords: Perforate, Three-port technique, Resistance, Grazing flow, Non-linear effects

1. Introduction

Perforated plates are an integral component of passive noise control solutions, e.g., aircraft liners and mufflers. Majority of the applications of a perforated plate involve an exposure to grazing flow and high-level acoustic incidence [1]. Aero-acoustic characterization of perforates is hence necessary and has been studied in detail over the last few decades [2, 3, 4, 5, 6]. The

current scientific discussion involves the effect of relative propagation and mean flow directions on the passive acoustic property of perforates. Various impedance eduction techniques on liners have shown differing results when the propagation is from either the upstream or downstream direction [6, 7]. Many of these techniques implement the Myers boundary condition [8] to explain the flow-acoustic interaction along the perforated surface, however, other studies like Renou and Auregan [9] also contradict this boundary condition. Hence there is a requirement of experimental results acquired without implementing any boundary condition to further the study of perforates.

Direct methods using impedance tubes as a sidebranch, and the in-situ method have also been popularly used on perforated facesheets by Dickey et al. [10] and Dean [11]. Inspired from these studies, this paper contributes to the ongoing research by providing experimental results of the perforate characteristics, namely the real part of the normalised transfer impedance and the scattering matrix. These characteristics are determined under excitation from three different directions with respect to the grazing flow.

Aero-acoustic characterization of circular and rectangular T-Junctions have been studied using the three-port technique, described in detail by Karlsson and Åbom [12] and Holmberg et al. [13], respectively. When compared against a grazing flow velocity based Strouhal number, an oscillating behaviour of amplification and attenuation of the incoming sound waves is observed. This behaviour is associated with hydrodynamic feedback, as also seen in Testud et al. [14], Moers et al. [15] and Howe [16].In this paper, following Karlsson and Åbom [12] and Holmberg et al. [13], the three-port technique is used to determine the acoustic properties of a perforated plate which is mounted at the intersection of a T-junction. The application of the technique is first carried out in Refs. [17, 18] and is further studied here. In absence of grazing flow the determined resistance of the perforate agrees well with the model proposed by Guess [5], where the model is scaled with respect to the discharge coefficient of the plate, as shown in Refs. [17, 18].

In presence of grazing flow, it was found in Ref. [17] that the Strouhal number at which, for an empty T-Junction the maximum amplification of incoming sound waves is seen, is the fifth harmonic of the Strouhal number at which the resistance of the perforate is minimum. This suggested a resemblance in the behaviour of an empty T-Junction and a perforate. However, the testing parameter range of the grazing flow velocity and the frequency did not experimentally validate this resemblance in Ref. [17]. In order to study if the behaviour of an empty T-junction and a perforated plate is anal-

ogous in nature, expansion of the testing conditions was carried out in Ref. [19]. It was found that in case of the perforate, an oscillating behaviour is absent. Instead, the Strouhal number of interest represents a limit till which the nature of the normalised resistance is dependent on both the flow- and the acoustic field, and beyond this Strouhal number, it is mainly depending on the acoustic field. Results from Kooi and Sarin [20], Cummings [21] and Kirby and Cummings [22] suggest that the determined resistance uptill the above-mentioned Strouhal number limit is dependent on the skin-friction velocity of the flow profile. For Strouhal numbers above the limit, Kooi and Sarin [20] suggest that the resistance is equal to the resistance determined in absence of grazing flow. Discussion of the above mentioned points is carried out in section 4.1.

In case of high-level excitation incidence, several studies have been carried out to determine the non-linear behaviour of the resistance, e.g., Refs. [3, 23, 24, 25, 26]. A majority of the existing research separately determines the non-linear part of the impedance and then adds it to the impedance determined in the linear range. A dependence of the non-linear part of the resistance on the in-hole particle velocity is observed in most of these models. In absence of grazing flow, Temiz et al. [27] propose a model for microperforated plates with circular orifices and sharp edges in the transition region where the Strouhal number, determined using the in-hole particle velocity, is close to a value of 1. This model is used as a reference for the three-port measurements as shown in Shah et al. [18], and agrees well for the majority of the frequency range used in the experiments. For a strongly non-linear regime, i.e., Strouhal number $\ll 1$, a deviation from the transition state model is seen and the resistance is found to be linearly dependent on the particle velocity. In presence of grazing flow, models proposed by Elnady and Bodén [28] and Renou [29] show the dependence of the non-linear part of the resistance on the in-hole particle velocity. However, for lower grazing flow speeds, Shah et al. [18] show that the non-linear part of the resistance has a 2^{nd} degree polynomial relationship with the ratio of in-hole particle velocity and the grazing flow velocity. The behaviour of this relationship is studied in further detail in this paper, as shown in section .

Experiments carried out on the perforate in the T-junction attempt to characterize the aero-acoustic field in the T-Junction, by comparing the real part of the normalised transfer impedance and the scattering matrix coefficients. Given that the perforate is studied under a plane wave excitation, the wavelength of the incoming sound waves is very high compared to the thick-

ness of the perforate. Hence only the real part of the transfer impedance, i.e., the resistance is considered in this study. Unlike a traditional liner, a relatively smaller surface area of the perforated plate is studied here. Hence, a negligible disruption of the flow profile is seen across the length of the perforated section. However, the results of the transfer impedance show a similarity with the trends observed in Kooi and Sarin [20], where the experiments were carried out on a lined section significantly larger than the one considered in this study. This suggests that the study of a smaller exposed area does not alter the aero-acoustic properties observed.

Based on the determined results, this paper proposes a semi-empirical model for the resistance in presence of grazing flow and high-level excitation. The proposed model includes the dependence on the flow profile characteristics of Mach number, as well as dimensionless numbers such as the Strouhal and the Shear number. Dependence on the perforate properties of thickness, diameter of perforation and open area are not included in the model and are only used to calculate the linear resistance in absence of grazing flow. This is not to contradict existing research that the resistance of the perforate in presence of grazing flow depends on these factors, but due to the study consisting of experiments on only one perforate sample. In addition, the coefficients describing the resistance of the perforate in Section 4 are determined empirically and can be dependent on the perforate properties.

2. Theoretical Background

The characterisation of the acoustic properties of perforated plates is generally done using the normalised transfer impedance ($\bar{Z}$) where the actual transfer impedance of the perforate is normalised with respect to the characteristic impedance of air. The other characteristic of interest is the three-port scattering matrix (S-Matrix). To avoid the experimental errors related to the standing wave pattern in the ducts, a correlation between the scattering matrix coefficients and the normalised transfer impedance is shown in Ref. [17]. The above-mentioned correlation defines the transfer impedance and is explained and governed by equations given in Section 3. A brief background of the existing research reviewed in this study is explained below.

2.1. Linear Resistance in absence of grazing flow

In Shah et al. [18], as well as in Ref. [17], the experimentally determined real part of normalised transfer impedance, i.e., the resistance ($\Re$) in absence

of grazing flow and in the linear range in the three-port setup, agrees well with the model shown in Eq.(1) [5, 28].

$$\Re = \frac{(\sqrt{8\nu\omega})t^{'}}{\sigma c d C_d} + \frac{\rho c d^2}{2\lambda^2},\ t^{'} = t + d, \tag{1}$$

where ν is the kinematic viscosity, ω is the angular frequency, σ is the percentage open area, c is the speed of sound, d is the diameter of the perforation, t is the thickness of the perforate, ρ is the density at room temperature, and λ is the excitation wavelength. The extended thickness ($t^{'}$) is defined as the sum of t and d by Guess [5]. The scaling with respect to the discharge coefficient (C_d) is as proposed by Elnady and Bodén [28]. Determination of C_d is done as shown in Shah et al. [18]. This value of resistance is used as a reference for calculating the resistance in presence of grazing flow as well under high-level excitation.

2.2. Non-Linear Resistance in absence of grazing flow

The non-linear part of the resistance calculated using the three-port measurements is investigated in Shah et al. [18]. The determined resistance at high-level excitation follows the model proposed by Temiz et al. [27]. The model is governed using an empirically defined function F_c, where F_c is determined using dimensionless Strouhal number (St_u) and Shear number (Sh). These dimensionless numbers are defined in Eq.(2).

$$\begin{aligned} Sh &= d\sqrt{\frac{\omega\rho}{4\mu}} \\ St_u &= \frac{\omega d}{u} \end{aligned}, \tag{2}$$

where μ is the dynamic viscosity, and u is the r.m.s. value of the in-hole particle velocity. For most of the frequency range the experimentally determined non-linear part of resistance ($\Re_{NL}$) follows Eq.(3).

$$\begin{aligned} \Re_{NL} &= \frac{F_c(St_u, Sh)\rho u}{2{C_v}^2\sigma} \\ F_c(St_u, Sh) &= \frac{1}{1 + 2St_u[1 + 0.06e^{3.74/Sh}]} \end{aligned}, \tag{3}$$

where C_v is the vena-contracta factor, which is taken to be 0.57 following Shah et al. [18]. The resistance under high-level excitation can be determined

with the addition of the non-linear part $\Re_{NL}$, and the resistance calculated in the linear range following Eq. (1). The validity of this model as per Temiz et al. [27] is said to be in the region of St_u $\mathcal{O}$ 1.

2.3. Linear Resistance in presence of grazing flow

Which grazing flow parameter best defines the relationship of the resistance in presence of grazing flow, is contested in the previous studies. Models proposed by Kooi and Sarin [20] and others [21, 22] discuss the dependence of the resistance on the skin friction velocity (u_τ) as well as frequency following Eq. (4).

$$\frac{\Re_{Flow} c}{\omega d} = \frac{\kappa u_\tau}{\omega d} - \zeta, \tag{4}$$

where $\Re_{Flow}$ is the resistance determined in presence of grazing flow and κ, ζ are empirically defined coefficients depending on the thickness of the perforate, and the diameter of the perforations. These constants differ in each reference. On the other hand, models proposed by Rao and Munjal [30] and others [3, 5] show the resistance to be a function of only the grazing flow Mach number (M), and independent of the frequency, following Eq.(5).

$$\Re_{Flow} = \frac{\epsilon M}{\sigma}, \tag{5}$$

where ϵ is also an empirically defined coefficient equal to 0.3 in Ref. [3, 5] and 0.53 in Ref. [30]. In Ref. [17] it is observed that the behaviour of the resistance determined in the three-port setup at different grazing flow velocities converges at a particular flow Strouhal number (St_U) defined using the flow velocity. This suggests a dependence of the resistance on this Strouhal number. To validate, experimental parameters, namely the frequency range and the grazing flow velocities are expanded in this paper and the determined resistance is discussed in Section 4. The definition of the flow velocity based Strouhal number is as per Eq.(6).

$$St_U = \frac{\omega d}{U}, \tag{6}$$

where U is the grazing flow bulk velocity.

2.4. Non-Linear Resistance in presence of grazing flow

The reviewed research, namely Feder and Dean [11], Dean [2], Elnady [28], and Renou [29] decouples the non-linear effects observed in the determined resistance in presence of high-level excitation and grazing flow from the flow parameters. They observe the non-linear effects to be solely dependent on the in-hole particle velocity of the perforate. However Shah et al. [18], based on experimental results at low grazing flow velocities (Mach number ≤ 0.05), shows that there exists a 2^{nd} degree polynomial relation between the non-linear part of the resistance ($\Re_{NL-Flow}$) and the ratio of particle velocity to the grazing flow velocity (u/U). The relationship follows Eq.(7).

$$\Re_{NL-Flow} = \alpha(\frac{u}{U})^2 + \beta(\frac{u}{U}) + \gamma, \tag{7}$$

where α,β,γ are the coefficients governing the relationship and their behaviour is discussed in the Section 4.

3. Experimental Technique

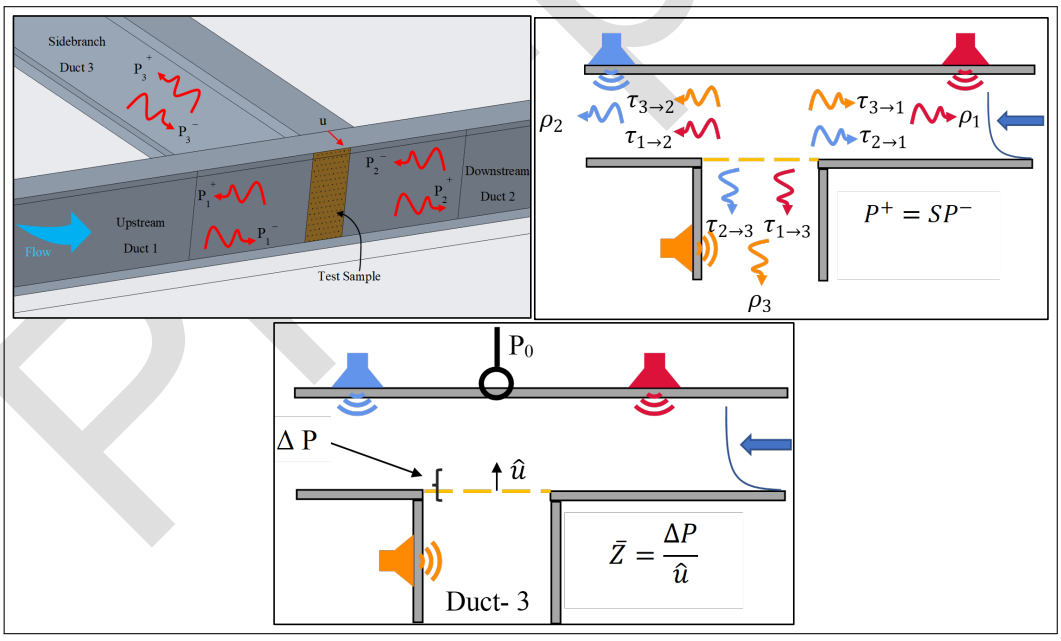

Fig. 1: (a) Schematic of the three-port technique; (b) Calculation of the scattering matrix; (c) Calculation of the transfer impedance

The schematic of the experimental setup is as shown in Fig.1-a. The perforate is flush mounted at the intersection of duct-1,2 and 3, where grazing flow is possible from duct-1 to 2. The end of duct-3 is sealed to have a net zero flow in the duct and avoid leakage. The three-port scattering matrix (S-Matrix) is as defined by Karlsson and Åbom [12]. The S-Matrix consists of reflection (ρ_x) and transmission coefficients ($\tau_{x\to y}$), and is determined with the help of the decomposed wave pressure amplitudes $P_{x\pm}$. It follows Eq.(8) and the nomenclature is as shown in Fig.1-b.

$$\begin{bmatrix} P_{1+} \\ P_{2+} \\ P_{3+} \end{bmatrix} = \begin{bmatrix} \rho_1 & \tau_{2\to1} & \tau_{3\to1} \\ \tau_{1\to2} & \rho_2 & \tau_{3\to2} \\ \tau_{1\to3} & \tau_{2\to3} & \rho_3 \end{bmatrix} \begin{bmatrix} P_{1-} \\ P_{2-} \\ P_{3-} \end{bmatrix} \tag{8}$$

The determination of the decomposed wave pressures is done using the multi-microphone method [31], where $P_{x\pm}$ are determined in each duct using acoustic pressures measured by three microphones in each duct. The propagating wavenumber (k) is determined using model proposed by Dokumaci [32]. To avoid errors pertaining to background noise a frequency response function between the measured pressure signal and the loudspeaker voltage is used for the analysis. In addition to the three microphones in each duct one more microphone is flush mounted on the wall opposite to the perforate and at the centre of the perforated section, i.e., at the intersection of duct-1, and -2. This microphone is used to acquire pressure P_0,as shown in Fig.1-c, and used to calculate the resistance.

The experimentally determined resistance is defined following Eq.(9). The nomenclature follows that of Fig.1-c.

$$\Re = \frac{1}{\rho c} real(\frac{\Delta P}{\hat{u}}) = real(\frac{P_3 - P_0}{P_{3-} - P_{3+}}), \tag{9}$$

where $\hat{u}$ is the particle velocity determined at the sample surface and is determined using the difference of decomposed pressure wave components in duct-3.

In Ref. [17] it is shown that the difference in the resistance determined using the total acoustic pressure P_0 measured by the microphone and the average of total acoustic pressures in duct-1 and -2, is negligible. Hence, we can assume that P_0 is equal to the average of total acoustic pressures P_1 and P_2. Additionally, assuming anechoic termination, a new formulation of the resistance is proposed that correlates the S-Matrix coefficients and the resistance. The usage of this formulation reduces the errors pertaining

to the standing wave pattern created in the three ducts, as the S-Matrix coefficients are independent of the termination reflections. The relation is shown in Eq.(10).

$$\begin{aligned} \Re_1 = &\quad real(\frac{\rho_1 + \tau_{1\to2} + 1}{2\tau_{1\to3}} - 1), \\ \Re_2 = &\quad real(\frac{\rho_2 + \tau_{2\to1} + 1}{2\tau_{2\to3}} - 1), \\ \Re_3 = &\quad real(\frac{1+\rho_3}{1-\rho_3} + \frac{\tau_{3\to1} + \tau_{3\to2}}{2(1-\rho_3)}), \end{aligned} \tag{10}$$

where $\Re_x$ is the resistance determined under excitation from duct-x.

For the determination of the non-linear part of the resistance, the controlling parameter chosen is the in-hole particle velocity, i.e., individual frequencies are chosen and the r.m.s. value of the in-hole particle velocity is increased from $\approx$ 1 m/s to $\approx$ 10 m/s. The calculation of the r.m.s. value of the in-hole particle velocity in SI units follows Eq.(11)

$$u = |\hat{u}|\frac{V_{rms}}{\rho c S_i \sigma}; V_{rms} = \sqrt{V_{AS} L_w}, \tag{11}$$

where V_{rms} is the r.m.s. value of the acoustic incidence auto spectra (V_{AS}), corrected with the Hanning window factor (L_w). To convert into the SI units, the sensitivity of the microphones (S_i) is divided. Lastly, to calculate the in-hole value, conservation of mass and isentropic nature is assumed and the value calculated at the surface is scaled with the porosity of the perforate (σ).

It is observed that in case of excitation from ducts-1, and 2, the particle velocity determined in duct-3 is limited due to the range of the loudspeakers used for excitation. Hence the S-Matrix cannot be determined for these higher velocity levels and the chosen frequencies, and the resistance is defined using Eq.(9). Additionally, it should be noted that the non-linear part of the resistance observed at lower in-hole particle velocity levels is found to be independent of incidence direction, as shown in Shah et al. [18]. Hence, only the resistance determined under excitation from duct-3 is studied here. For the linear cases, the controlling parameter is the level of excitation incident on the perforate and the resistance is determined across a wider frequency range, increasing the experimental errors related to the standing wave pattern and hence it follows the definition from Eq.(10), reducing this error.

The sample studied here is a rectangular perforate with circular perforations and square edges, with a 2.54% open area. The diameter of the perforation and the plate thickness are both 1.2 mm and the rectangular T-junction has a cross section of 25 mm by 120 mm. The acoustic pressure was acquired using calibrated flush mounted microphones of type Brüel and Kjær $\frac{1}{4}$- inch 4938. NI 9234 DAQ modules were used for data acquisition at a sampling frequency of 25.6 kHz. Plane wave propagation is assumed and the frequency range of the measurements (100-2250 Hz) as well as the microphone distances were determined following the recommendations of Åbom and Bodén [33]. Static temperature measured by a calibrated K-type thermocouple placed in duct-3 is used for determining the speed of sound and further post-processing of acquired data. The determination of the skin friction velocity and the grazing flow bulk velocity follows the method explained in Ref. [17]. The grazing flow bulk velocity is calculated by integrating the flow profile across half the duct width. The average ratio of the calculated bulk velocity to the maximum grazing flow velocity, i.e., the flow velocity measured at the centre of the duct cross-section is found to ≈ 0.92. Additionally, negligible deviation of the flow profile is observed over the perforated region, as shown in Ref.[17]. During the acoustical measurements, a simultaneous flow profile determination was not possible, hence the bulk velocity which is used for post-processing is calculated by multiplying 0.92 with grazing flow velocity measured at the centre of the cross-section, upstream of the sample. The flow rig was controlled to measure the acoustic properties in the range of the bulk velocity from ≈ 10 m/s to ≈ 60 m/s. Stepped sine excitation was used and a signal-to-noise ratio of at least 20 dB was maintained for all the measurements.

4. Results and Discussion

The following section discusses the behaviour of the resistance of the perforate in presence of grazing flow and high-level excitation. The first subsection discusses the comparison of the resistance in the linear range with existing models [5, 20, 28]. Additionally, beyond the experimental range of Kooi and Sarin [20], deviation of the experimental results from their proposed model is investigated. Then, a semi-empirical model covering the entire operating range is proposed. In subsection 4.2, the experimental results in absence of grazing flow are presented and shown to agree with Temiz et al.'s model [27]. In presence of grazing flow, results from Shah et al. [18] are

further studied and the relation between the non-linear part of the resistance and the in-hole particle velocity, grazing flow velocity and the Shear number is discussed.

4.1. Resistance in the linear range

The resistance of the perforate in the linear regime was determined experimentally with and without grazing flow, and the results were compared with some existing models. The comparison is shown in Fig.2. Fig.2-a shows the no grazing flow case, where the determined resistance agrees with the model proposed in Eq.(1). A deviation is observed at $\approx$ 1400Hz. However, the deviation does not represent the property of a sample but is present due to the presence of a pressure anti-node at one of the microphone locations. The anomaly disappears on the addition of grazing flow as the entire standing wave pattern changes. Apart from the deviation a good agreement is observed between the model and the experimental results in absence of grazing flow.

In Fig.2 -b to -f, results determined at different grazing flow velocities are shown, along with the resistance modelled as a function of the skin-friction velocity and the frequency, as per Eq. (4). As mentioned in Section 2, the value of the empirical coefficient κ varies in different studies. Here, to show the comparison of the nature of the resistance, κ is interpolated at each flow velocity to get a good match with the experimental results. For the lower flow velocities, i.e., Fig.2 -b and -c, the frequency at which the model starts differing from the results corresponds to $St_U \approx 0.7$. $St_U \approx 0.7$ matches the limit of $u_\tau/fd \approx 0.2$, beyond which Kooi and Sarin [20] propose that their model is valid. Kooi and Sarin [20] state for higher values of St_U, the flow induced resistance is negligible and that the resistance in presence of grazing flow can be determined following the models proposed for the no grazing flow case, which is not seen here. The resistance for $St_U > 0.7$ is still found to be dependent on the grazing flow Mach number.

Moreover, the model also does not account for the difference observed in resistance when the excitation is in the flow direction ($\Re_1$), and when it is against it ($\Re_2$), as observed at higher flow velocities, e.g., in Fig.2 -e and -f. Lastly, looking at the experimental results in Fig.2 -e and -f, it would be not be an unfair assumption to state that the resistance is independent of the frequency, suggesting the behaviour followed by models in Eq.(5) [3, 5, 30], and the validity of these studies.

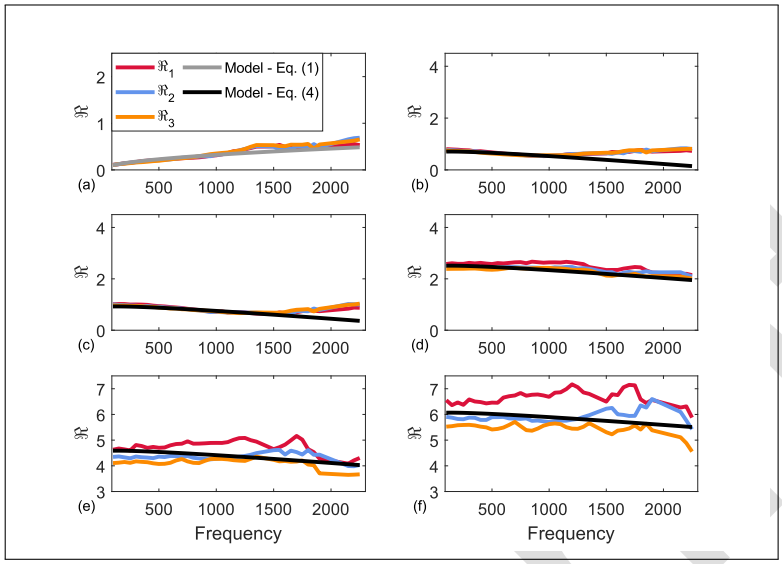

Fig. 2: Comparison of resistance determined following Eq.(10) in the three-port setup, with existing models against frequency. a) No grazing flow; b) Grazing flow $M \approx 0.03$; c) Grazing flow $M \approx 0.04$; d) Grazing flow $M \approx 0.08$; e) Grazing flow $M \approx 0.13$; f) Grazing flow $M \approx 0.17$.

To observe the resistance at a comparable value at all the flow velocities, the scaling of the resistance is applied. It is found that when the resistance is scaled with respect to $M^{1.17}(1 + St_U)^{1.75}$, all the curves at different flow velocities collapse well with each other. Moreover, to account for the difference in the resistance observed with respect to the relative incidence and flow direction, an additional numerical scaling factor can be used to make the resistance independent of the incidence direction. In this study the scaling factors are 0.92 for $\Re_2$ and 0.85 for $\Re_3$. These scaling factors are determined empirically and the combined scaling is done following Eq.(12).

$$\begin{aligned} \Re_1' &= \frac{\Re_1}{M^{1.17}(1+St_U)^{1.75}}, \Re_2' = \frac{\Re_2}{0.92M^{1.17}(1+St_U)^{1.75}}, \\ \Re_3' &= \frac{\Re_3}{0.85M^{1.17}(1+St_U)^{1.75}}, \end{aligned} \tag{12}$$

Fig.3 and Fig.4 show the scaled value of resistance at 12 different grazing flow velocities compared against the flow velocity governed Strouhal number (St_U). As observed in Refs. [17, 19], the behaviour of the resistance before

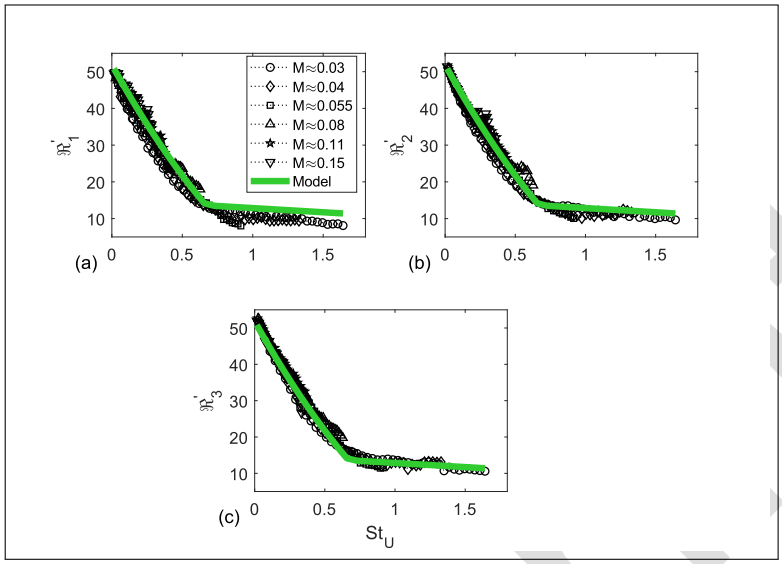

Fig. 3: Comparison of resistance determined in presence of certain grazing flow velocities and scaled following Eq.(12) (black points) with model proposed in Eq.(13) (green lines), against flow velocity governed Strouhal number. Resistance determined under excitation from: (a) duct-1; (b) duct-2; (c) duct-3.

and after the limit of $St_U \approx 0.7$ is completely different. For the lower St_U region, the relation between the scaled value of resistance and St_U is a 2^{nd} degree polynomial. However, after the limit the relation becomes linear with respect to St_U. Moreover, for $St_U > 0.7$, an additional linear dependence on the Mach number is also observed. Hence, a model using empirical defined coefficients can be used to define the resistance in presence of grazing flow in terms of St_U and M. It is displayed in Eq.(13) and the comparison with experimental results is shown in Fig.3 and Fig.4.

$$\Re_x = \begin{cases} when\ St_U < 0.7 & \frac{1}{\psi} M^{1.17}(1+St_U)^{1.75}(17.94{St_U}^2 - 69.22St_U + 51.86) \\ when\ St_U > 0.7 & \frac{1}{\psi} M^{1.17}(1+St_U)^{1.75}((-440M + 10.93)St_U + 311M + 5.8)' \end{cases} \tag{13}$$

where ψ= 1 for $\Re_1$, 0.92 for $\Re_2$, and 0.85 for $\Re_3$.

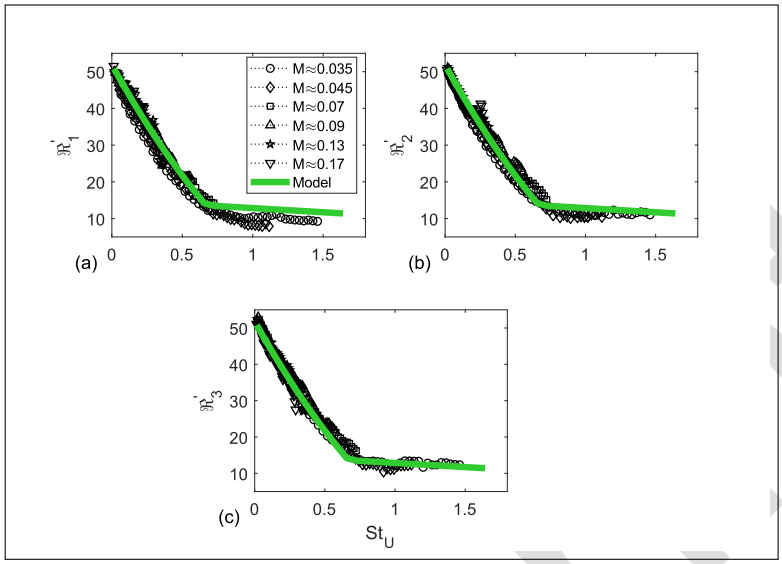

Fig. 4: Comparison of resistance determined in presence of different grazing flow velocities and scaled following Eq.(12) (black points) with model proposed in Eq.(13) (green lines), against flow velocity governed Strouhal number. Resistance determined under excitation from: (a) duct-1; (b) duct-2; (c) duct-3.

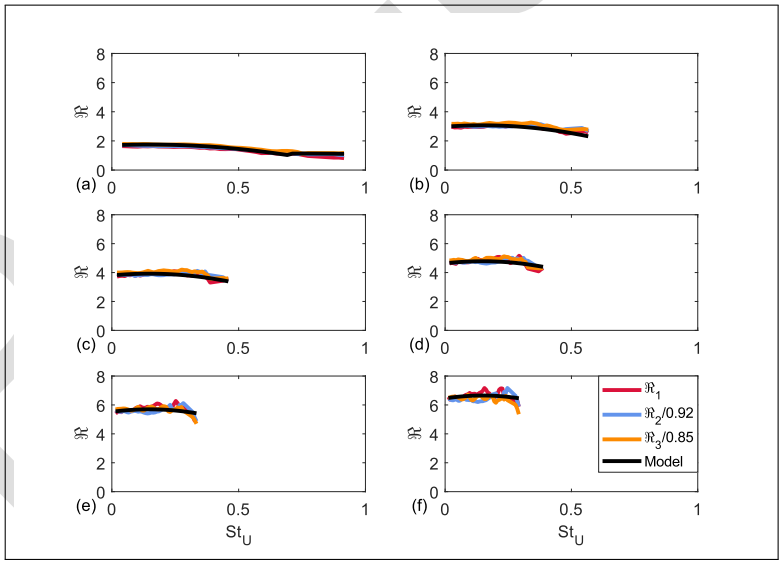

Fig. 5: Comparison of determined resistance, scaled as per the legend, with the model proposed in Eq.(13) against the flow velocity governed Strouhal number. (a) Grazing flow $M \approx 0.055$; (b) Grazing flow $M \approx 0.09$; (c) Grazing flow $M \approx 0.11$; (d) Grazing flow $M \approx 0.13$; (e) Grazing flow $M \approx 0.15$; (f) Grazing flow $M \approx 0.17$.

Fig.5 shows the comparison of the experimentally determined resistance at higher flow velocities ($M > 0.05$) against the Strouhal number. The normalised resistance from different incidence directions is scaled with ψ, following Eq. (13). The experimental results are compared with the model of $\Re_1$ from Eq.(13) and a good agreement can be seen.

4.2. Resistance under high-level excitation

Extending the results of Shah et al.[18] the non-linear part of resistance is studied with and without grazing flow. Comparison between the experimental results with the model proposed by Temiz et al. [27] against $1/St_u$ is as shown in Fig.6. The model is seen to be in good agreement with the results for $1/St_u <\approx 3$. For $1/St_u > 3$, the transition state model no longer matches the results, where the experimental results show the resistance to be linearly dependent on the in-hole particle velocity, as is observed in Melling [4]. In case of 1100 Hz, experimental results deviate from the model at one particle velocity levels. The deviation can be due to the experimental errors as the hardware limits of the loudspeaker were reached in increasing the particle velocity at higher frequencies.

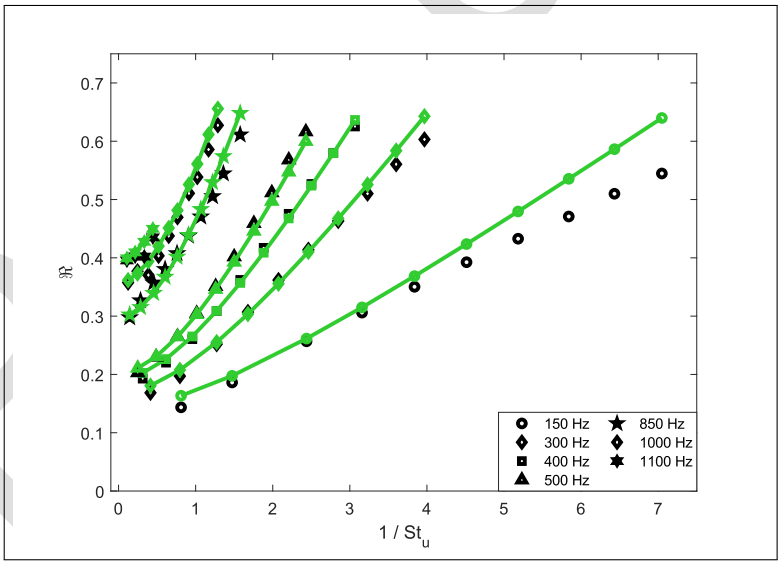

Fig. 6: Comparison of the resistance in absence of grazing flow and under high-level excitation with existing model following Eq.3 (green lines), against the in-hole particle velocity governed inverse Strouhal number.

In presence of grazing flow, the non-linear part of the resistance is determined at flow velocities of $M \approx 0.03$, 0.04 and 0.05. In Shah et al. [18] the behaviour of this resistance is shown to be governed by the ratio of in-hole particle velocity and grazing flow velocity (u/U) and follows Eq.(7). The experimentally determined value of non-linear part of resistance is shown in Fig.8 and Fig.9.

To further study the behaviour of the coefficients in Eq.(7), they are interpolated to match with the experimental results. Fig.7 shows the interpolated value of the coefficients at two different flow velocities, namely when $M \approx 0.03$, and 0.04, compared against the dimensionless ratio of Shear number and grazing flow Mach number (Sh/M). The values of these interpolated coefficients shows a linear relationship with the Sh/M ratio,

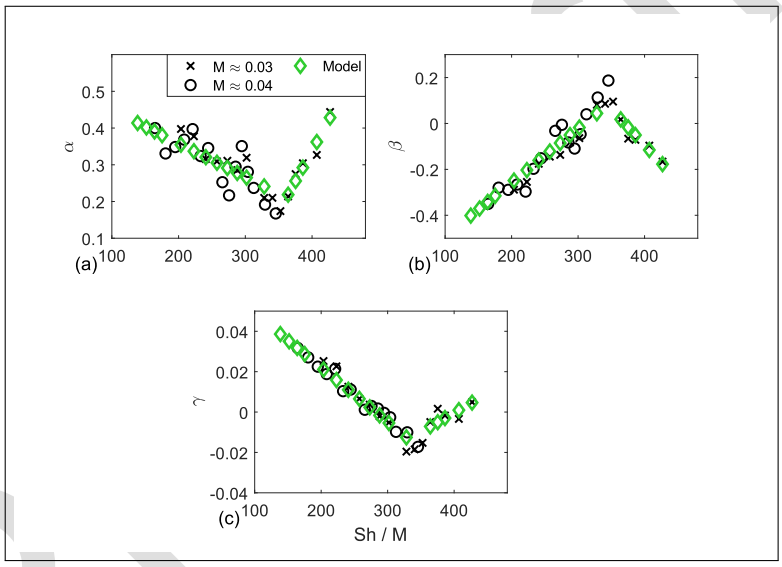

Fig. 7: Comparison of the value of the interpolated polynomial coefficients governing the non-linear part of the resistance in presence of grazing flow with model proposed in Eq. 14, against a ratio of Shear number and grazing flow Mach number. (a) Value of α; (b) Value of β; (c) Value of γ;

It can be observed that the behaviour of the interpolated coefficients completely opposite before and after the ratio of Sh/M reaches a value of ≈ 344. This is also the numerical value of the speed of sound at the in-duct temperatures. This observation, and the definition of Shear number suggests that the onset of the positive $\Re_{NL-Flow}$ values is dependent on the oscillating Stoke layer thickness and the displacement generated by the grazing flow.

This relationship of the α, β, and γ values with Sh/M is quantified in Eq.(14).

$$\begin{aligned} when\ Sh/M <\approx 344; \quad & \begin{matrix} \alpha \\ \beta \\ \gamma \end{matrix} = \begin{cases} -9.1X10^{-4}(Sh/M) + 0.54 \\ 2.3X10^{-3}(Sh/M) - 0.73 \\ -2.7X10^{-4}(Sh/M) + 0.076 \end{cases}, \\ when\ Sh/M >\approx 344; \quad & \begin{matrix} \alpha \\ \beta \\ \gamma \end{matrix} = \begin{cases} 3.3X10^{-3}(Sh/M) - 0.99 \\ -3.1X10^{-3}(Sh/M) + 1.15 \\ 1.9X10^{-4}(Sh/M) - 0.075 \end{cases} \end{aligned} \tag{14}$$

Incorporating these coefficients in Eq.(7), the non-linear part of resistance is determined in presence of grazing flow and compared with the proposed model in Fig.8 and Fig.9. A good agreement between the model and the experiments is observed at lower flow velocities.

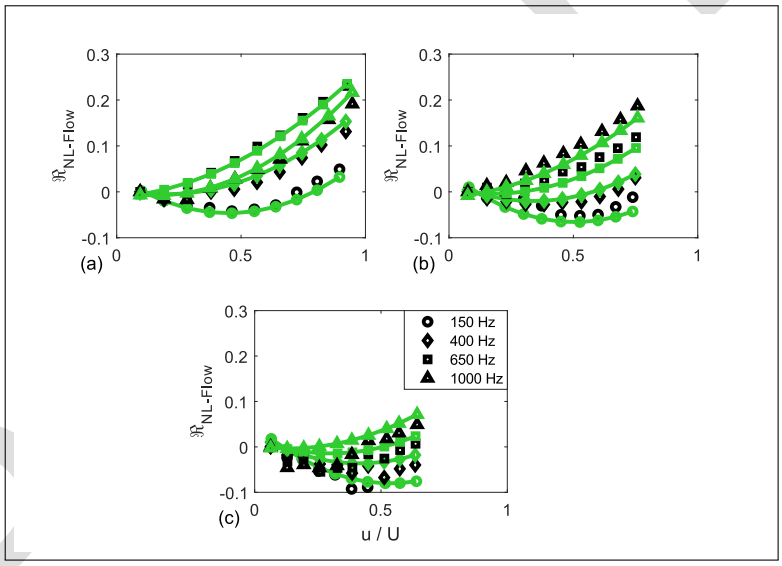

Fig. 8: Comparison of the experimentally determined non-linear part of resistance at selected frequencies (black points) in presence of grazing flow with proposed model following Eq.(7) (green lines), against ratio of in-hole particle velocity and grazing flow bulk velocity. (a) Grazing flow $M \approx 0.03$; (b) Grazing flow $M \approx 0.04$; (c) Grazing flow $M \approx 0.05$

The outlier in Fig.9 is the case of 850 Hz and the grazing flow velocity of $M \approx 0.05$. For that frequency, the value of the non-linear part of the resistance remains almost constant at lower values of u/U and the deviation is not repeated at other frequencies or flow velocities, suggesting a presence

of an experimental error due to the shifting of the standing wave pattern and the presence of antinodes at the microphone location.

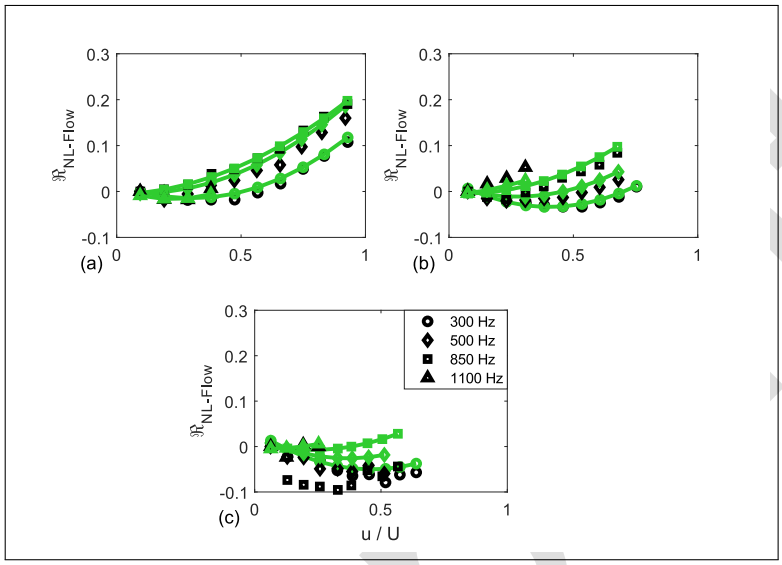

Fig. 9: Comparison of the experimentally determined non-linear part of resistance at different frequencies (black points) in presence of grazing flow with proposed model following Eq.(7) (green lines), against ratio of in-hole particle velocity and grazing flow bulk velocity. (a) Grazing flow $M \approx 0.03$; (b) Grazing flow $M \approx 0.04$; (c) Grazing flow $M \approx 0.05$

Combining the effects of grazing flow (Eq.(13)) and high-level excitation (Eq.(7) and Eq.(14)), an entire model can be proposed for the resistance of the perforate. In Fig.10, the results following such a model are compared with the experimentally determined resistance at three grazing flow velocities and two in-hole particle velocity levels.

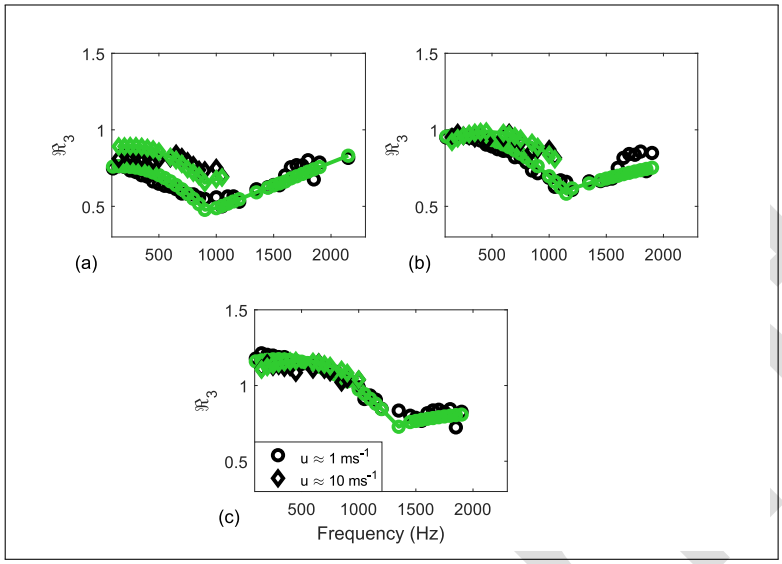

Fig. 10: Comparison of the resistance under excitation from duct-3 in presence of grazing flow at different in-hole particle velocity levels with combined model (green lines), against frequency. (a) Grazing flow $M \approx 0.03$; (b) Grazing flow $M \approx 0.04$; (c) Grazing flow $M \approx 0.05$

5. Concluding Remarks

This paper provides an insight into the usage of a novel direct method for the transfer impedance determination of a perforate, namely the three-port technique. The normalised resistance, a passive acoustic property of the perforate in presence of grazing flow and high-level excitation is studied, and experimental results are provided. Behaviour of the determined resistance is classified into two regions based on the grazing flow velocity Strouhal number. Based on the results a model is proposed which correlates the resistance with the Strouhal-, and the Mach number. The empirically determined coefficients of the equation and their dependence on the perforate properties like porosity, thickness and perforation diameters can be further studied. Under high-level excitation, dependence of resistance on the in-hole particle velocity, grazing flow velocity and shear number is shown and a relation to calculate the non-linear effect at low grazing flow velocities is shown. Lastly, experimental results under both grazing flow and high level excitation are compared with the models and agreement is shown.

Acknowledgments

This work is part of the Marie Skłodowska-Curie Initial Training Network Pollution Know-How and Abatement (POLKA). We gratefully acknowledge the financial support from the European Commission under call H2020-MSCA-ITN-2018 (project number: 813367).

References

[1] H. Bodén, L. Zhou, J. Cordioli, A. Medeiros, A. Spillere, On the effect of flow direction on impedance eduction results, in: in 22nd AIAA/CEAS Aeroacoustics Conference, 2016.

[2] P. Dean, An in-situ method of wall acoustic impedance measurements in flow ducts, Journal of Sound and Vibration 34 (1974) 97–130.

[3] E. Rice, A model for the acoustic impedance of a perforated plate liner with multiple frequency excitations, Report NASA TM-X-67950, NASA Technical Memorandum (1971).

[4] T. Melling, The acoustic impedance of perforates at medium and high sound pressure levels, Journal of Sound and Vibration (1973).

[5] A. Guess, Calculation of perforated plate liner parameters from specified acoustic resistance and reactance, Journal of Sound and Vibration 40 (1975) 119–137.

[6] M. Jones, W. Watson, B. Howerton, S. Busse-Gerstengarbe, Comparative study of impedance eduction methods, part 2: Nasa tests and methodology, in: 19th AIAA/CEAS Aeroacoustics Conference, 2013.

[7] L. Zhou, H. Bodén, C. Lahiri, F. Bake, E. L, E. T., Comparison of impedance eduction results using different methods and test rigs, in: in 20th AIAA/CEAS Aeroacoustics Conference, 2014.

[8] M. Myers, On the acoustic boundary condition in the presence of flow, Journal of Sound and Vibration 71 (1980) 429–434.

[9] Y. Renou, Y. Aurégan, Failure of the ingard–myers boundary condition for a lined duct: An experimental investigation, The Journal of the Acoustical Society of America 130 (2011) 52–60.

[10] N. Dickey, A. Selamet, M. Ciray, An experimental study of the impedance of perforated plates with grazing flow, Journal of Acoustical Society of America 110 (2001) 2360–2370.

[11] E. Feder, L. W. Dean, Analytical and experimental studies for predicting noise attenuation in acoustically treated ducts for turbofan engines nasa contractor report cr-1373, Report, NASA Technical Memorandum (1969).

[12] M. Karlsson, M. Åbom, Aeroacoustics of t-junctions-an experimental investigation, Journal of Sound and Vibration 329 (2010) 1793–1808.

[13] A. Holmberg, M. Karlsson, M. Åbom, Aeroacoustics of rectangular t-junctions subject to combined grazing and bias flows - an experimental investigation, Journal of Sound and Vibration 340 (2015) 152–166.

[14] P. Testud, Y. Aurégan, P. Moussou, A. Hirschberg, The whistling potentiality of an orifice in a confined flow using an energetic criterion, Journal of Sound and Vibration 325 (2009) 769–780.

[15] E. Moers, D. Tonone, A. Hirschberg, Strouhal number dependency of the aero-acoustic response of wall perforations under combined grazing-bias flow, Journal of Sound and Vibration 389 (2017) 292–308.

[16] M. Howe, The dissipation of sound at an edge, Journal of Sound and Vibration 70 (1980) 407–411.

[17] S. Shah, H. Bodén, S. Boij, M. D'elia, Three-port measurements for determination of the effect of flow on the acoustic properties of perforates, in: AIAA Aviation 2021 Forum, 2021.

[18] S. Shah, H. Bodén, S. Boij, Nonlinear three-port measurements for the determination of high-level excitation effects on the acoustic properties of perforates, in: 28th AIAA/CEAS Aeroacoustics Conference, 2022.

[19] S. Shah, H. Bodén, S. Boij, Flow acoustic interaction in a rectangular t-junction with mounted perforate using acoustic three-port measurements (to be published), in: 51st International Congress and Exposition on Noise Control Engineering, 2022.

[20] J. Kooi, S. Sarin, An experimental study of the acoustic impedance of helmholtz resonator arrays under a turbulent boundary layer, in: 7th AIAA Aeroacoustics Conference, 1981.

[21] A. Cummings, The effects of grazing turbulent pipe-flow on the impedance of an orifice, Acoustica 61 (1986) 233–242.

[22] R. Kirby, A. Cummings, The impedance of perforated liners subjected to grazing flow and backed by porous media, Journal of Sound and Vibration (1998).

[23] I. Sivian, Acoustic impedance of small orifices, Journal of the Acoustical Society of America 7 (1935).

[24] U. Ingård, H. Ising, Acoustic nonlinearity of an orifice, Journal of the Acoustical Society of America 42 (1967).

[25] H. Bodén, One-sided multi-port techniques for characterisation of induct samples with nonlinear acoustic properties, Journal of Sound and Vibration 331 (2012).

[26] J. Betts, Experiments and impedance modeling of liners including the effect of bias flow, Thesis, Virginia Polytechnic Institute and State University (2000).

[27] M. Temiz, J. Tournadre, I. Arteaga, A. Hirschberg, Non-linear acoustic transfer impedance of micro-perforated plates with circular orifices, Journal of Sound and Vibration (2016).

[28] T. Elnady, H. Bodén, On the modelling of the acoustic impedance of perforates with flow, in: 9th AIAA/CEAS Aeroacoustics Conference, Vol. AIAA 2003-3304, 2003.

[29] Y. Renou, Impédance des traitements acoustiques absorbants en conduit : effets de l'écoulement rasant et de la couche limite, Thesis, Le Mans University (2010).

[30] N. Rao, M. Munjal, Experimental evaluation of impedance of perforates with grazing flow, Journal of Sound and Vibration (1986).

[31] A. Holmberg, M. Åbom, H. Bodén, Accurate experimental two-port analysis of flow generated sound, Journal of Sound and Vibration 330 (26) (2011) 6336–6354.

[32] E. Dokumaci, A note on transmission of sound in a wide pipe with mean flow and viscothermal attenuation, Journal of Sound and Vibration 208 (1997) 653–655.

[33] M. Åbom, H. Bodén, Error analysis of two-microphone measurements in ducts with flow, The Journal of the Acoustical Society of America 83 (1988).